Advances in Concrete Construction, *Vol. 10, No. 6 (2020) 537-546*
DOI: https://doi.org/10.12989/acc.2020.10.6.537

Combined effect of lightweight fine aggregate and micro rubber ash on the properties of cement mortar

Omar Mohamed Omar Ibrahim*[1,2] and Bassam A. Tayeh[3]

[1]*Department of Civil Construction and Architecture, Faculty of Technology and Education, Suez University, Suez, Egypt*
[2]*Higher Institute for Engineering and Technology At ElManzala, Ad Daqahliyah, Egypt*
[3]*Civil Engineering Department, Faculty of Engineering, Islamic University of Gaza, Gaza, Palestine*

(*Received August 15, 2020, Revised November 1, 2020, Accepted November 3, 2020*)

Abstract. Exterior walls in buildings are exposed to various forms of thermal loads, which depend on the positions of walls. Therefore, one of the efficient methods for improving the energy competence of buildings is improving the thermal properties of insulation plaster mortar. In this study, lightweight fine aggregate (LWFA) and micro rubber ash (MRA) from recycled tires were used as partial replacements for sand. The flow ability, unit weight, compressive strength, tensile strength, thermal conductivity (K-value), drying shrinkage and microstructure scan of lightweight rubberized mortar (LWRM) were investigated. Ten mixtures of LWRM were prepared as follows: traditional cement mortar (control mixture); three mixes with different percentages of LWFA (25%, 50% and 75%); three mixes with different percentages of MRA (2.5%, 5% and 7.5%); and three mixes consisting both types with determined ratios (25% LWFA+5% MRA, 50% LWFA+5% MRA and 75% LWFA+5% MRA). The flow ability of the mortars was 22±2 cm, and LWRM contained LWFA and MRA. The compressive and tensile strength decreased by approximately 64% and 57%, respectively, when 75% LWFA was used compared with those when the control mix was used. The compressive and tensile strength decreased when 5% MRA was used. By contrast, mixes with determined ratios of LWFA and MRA affected reduced unit weight, K-value and dry shrinkage.

Keywords: lightweight; rubber; mortar; thermal conductivity; shrinkage

1. Introduction

Solid wastes have caused a worldwide environmental concern. Among the cheap and simple methods for disposing tires are burning and dumping in massive landfills, but these methods cause severe environmental problems, and it is reported that a decrease in the properties of concrete, especially mechanical properties, occurs when rubber content increases (Mohamadien *et al.* 2019, Topçu 1995, Albano *et al.* 2005, Khaloo *et al.* 2008). The global consumption of rubber grew from 14.5 million tons to 14.6 million tons in 2012 and 2019, respectively (Alaloul *et al.* 2020, MREPCS 2019*)*. Tire burning generates dangerous gases and has thus deemed illegal by many countries, and storing tires is unhealthy because landfills are suitable environments for bacteria and insects. Hence, alternative methods and green solutions are needed (Sofi 2018, Najim and Hall 2012, Alaloul *et al.* 2020). Feasible solutions include recycling waste rubber and utilizing construction materials, and the reduction of pollution, carbon emissions and energy consumption have become a global movement (Hunag *et al.* 2015, Yu and Zhu 2016). Using waste rubber tires as building additives is considered a potential solution because waste tires cause intractable environmental, aesthetic and health problems (Yu and Zhu 2019).

One of the active methods to better the energy efficiency of construction buildings is to enhancement the thermal properties of insulation cement mortar. Insulation cement mortar is generally used on the exterior and interior wall of construction buildings, and it is cementitious material made of Portland cement, sand and various types of additives. An effective way to enhance the insulation mortar thermal properties is to use phase change materials (PCM) and recycled waste rubber particles such as scrap tires as additions (Pania *et al.* 2012, Saber 2012, Li and Li 2007). The walls are exposed to different forms of thermal loads, which vary according to the positions of the walls. Some walls are exposed to heat through natural or forced convection. After repeated thermal exposure, walls are subjected to thermal fatigue, which promotes crack formation and gap enlargement that finally leads to a fast K-value (Tarabieh and Aboulmagd 2019, Jie *et al.* 2019). Using PCM in mortar requires special manpower and is thus expensive (Richardson *et al.* 2017). Therefore, cheap alternative materials, such as lightweight materials, are necessary for reducing the thermal conductivity of mortar incorporating rubber waste materials. Cement mortar is mostly used in ornamentation art for ground, roof, exterior wall and interior wall surfaces (Sharkawi 2015). Lightweight mortar were achieved in a previous study (Ali *et al.* 2013) by using crushed red bricks or demolition waste or by improving some desirable properties, such as thermal properties, and the lowest weight was approximately 600 kg/m^3. The K-value of rubberized mortar decreases when crumb rubber with 28%, #10-20 was

*Corresponding author, Ph.D.
E-mail: omar.ibrahim@suezuniv.edu.eg

ISSN: 2287-5301 (Print), 2287-531X (Online)

Table 1 Chemical composition of cement

Constituent	SiO_2	Fe_2O_3	Al_2O_3	CaO	MgO	Na_2O	K_2O	SO_3
Composition %*	21.35	2.95	6.05	62.05	4.03	0.37	0.35	2.04

*The data were obtained by the manufacturer datasheet

Table 2 Physical properties of ordinary Portland cement

Property		Results	Specifications Limits
Compressive Strength of Standard Mortar (MPa)	3 days	22.1	Not less than 18**
	28 days	38.5	Not less than 36**
Fineness in Terms of S.S.A** (cm^2/gm)		3185	>2750**
Setting Time (min)	Initial	128	Not less than 45**
	Final	175	Not more than 600**

**Limits of EC 203-2016

used (Fadiel *et al.* 2014). Although significant work has been conducted on investigating the mechanical properties of used crumb rubber in cement composites (Fadiel *et al.* 2014), few studies have focused on the K-value. Thus, this research aims to develop a lightweight aggregate with a low K-value from waste and cheap materials and resolve environmental, energy and decoration problems. Firstly, the impact of lightweight fine aggregate (LWFA) at 25%, 50% or 75% ratio as a replacement for natural sand was investigated. Secondly, the study inspects the impact of micro rubber ash (MRA) at 5%, 2.5% or 7.5% as a partial substitute for natural sand in cement mortar. Thirdly, the impact of MRA and LWFA in determined ratios (25% LWFA+5% MRA; 50% LWFA+5% MRA and 75% LWFA+5% MRA) were explored. Fourthly, the fresh, physical and mechanical properties, such as flow ability, compressive and tensile strength; unit weight; thermal conductivity; shrinkage; and microstructure scan of cement mortar were tested.

2. Materials and methods

2.1 Materials

2.1.1 Cement

Ordinary Portland cement (OPC), CEM I 42.5N, was produced by the Suez Cement Company (Egypt). Fig. 1(a) illustrates the OPC. Cement tests were performed according to ASTM-C-150 and Egyptian Standard Specification (ESS) 4756-1/2009. The chemical compositions and physical properties of OPC are provided in Tables 1 and 2, respectively.

Table 3 Physical properties of used natural sand, LWFA and MRA

Property	Results			Limits*
	Natural Sand	LWFA	MRA	
Specific Weight	2.65	0.90	0.97	2.5-2.75
Bulk Density (t/m3)	1.76	0.50	0.528	----------
Water Absorption (%)	1.75	14.0	-------	Not more than 2.5
Clay and Fine Dust Content (% By Volume)	0.87	0.05	-------	Not more Than 3
Los Angles Abrasion Loss (%)	11.56	50.80	-------	Not more than 30

**Limits of EC 203-2016

Table 4 Grading of used natural sand and LWFA

Sieve size (mm)	9.5	4.75	2.36	1.18	0.6	0.3	0.15
Passing % for Used Natural Sand	100	100	95.3	85.95	65.95	35.61	10.62
Passing % for Used LWFA	99.1	91.2	69.67	45.95	30.95	15.61	8.62
Specification Upper Limits%	100	100	100	100	100	70	20
Specification Lower Limits %	100	89	60	30	15	5	0

2.1.2 Natural sand

Natural sand (NS) complies with ASTM C897-15 and Egyptian Code (EC) 203-2016 standards. The physical properties of used sand and sieve analysis results are provided in Tables 3 and 4, respectively. Fig. 2 presents the grading curve of sand, and Fig. 1(b) illustrates natural sand.

2.1.3 Lightweight fine aggregate

Lightweight fine aggregate (LWFA) was obtained from the coasts of El-Arish Governorate, Egypt. Fig. 1(c) illustrates the LWFA. The LWFA was drenched in tap water then washed with tap water several times for the reduction of chlorides and sulphate contents, mashed through ball milling and finally sieved using 0-4 mm sieves. The resulting Lightweight fine aggregate was used in manufacturing mortar mixtures. The produced LFWA met the requirements of EC 203-2016. The physical properties of the LWFA and sieve analysis results are provided in Tables 3 and 4, respectively. Fig. 2 presents the grading

(a) Cement (b) Natural Sand (c) Lightweight Fine Aggregate (d) Micro Rubber Ash

Fig. 1 Used materials

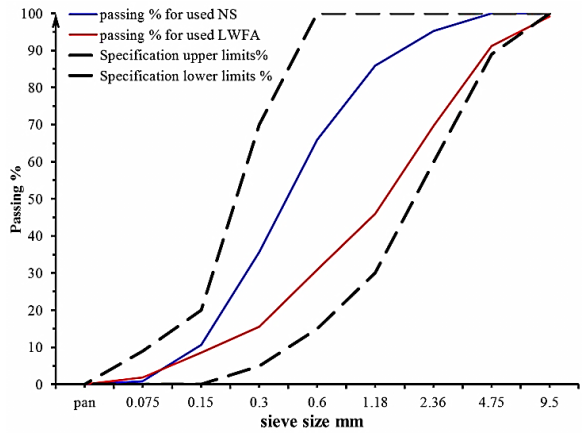

Fig. 2 Grading curves of used natural sand and LWFA

Table 5 Chemical analysis of used MRA

Chemical Composition*	Content %
Acetone Extract	14.85
Industrial Fabrics	4.65
Carbon black	30.28
Rubber hydrocarbon	50.15

*Chemical composition provided by the supplier

Table 6 Technical data of super-plasticiser

Property	Technical Data
Colour	Dark brown liquid
State	Liquid solution
Specific Gravity	1.2
Chloride Content	Nil
Compatibility with Cement	All kinds of Portland cement

curve of LWFA, and Fig. 3 illustrates the microstructure of LWFA.

2.1.4 Micro rubber ash

Micro rubber ash (MRA) was supplied by the (M-A-R-S-O) company. The sizes of MRA ranged from 12 µm to 45 *µm*, as shown in Fig. 4. The physical properties and chemical compositions of MRA are provided in Tables 3 and 5, respectively. MRA has a dark colour and a specific surface area of 1.54 m^2/g. Fig. 1(d) illustrates the MRA**.**

2.1.5 Admixture

A high-range naphthalene-sulphonated superplasticiser was used to enhance the workability of fresh mortar according to ASTM C494-80 types A and F. The superplasticiser was added at a percentage of 3% of cement weight. The technical data of superplasticiser is presented in Table 6.

2.2 Mix proportions

Table 7 shows the mix proportions of lightweight rubberized mortar (LWRM). Trial mixes were prepared in the laboratory and used in determining the limits of the contents of the materials and preparing lightweight mortar mixtures. The effects of the different proportions of LWFA

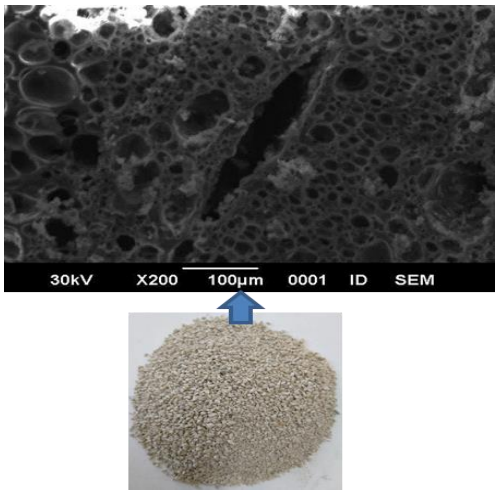

Fig. 3 Microstructures of lightweight fine aggregate LWFA

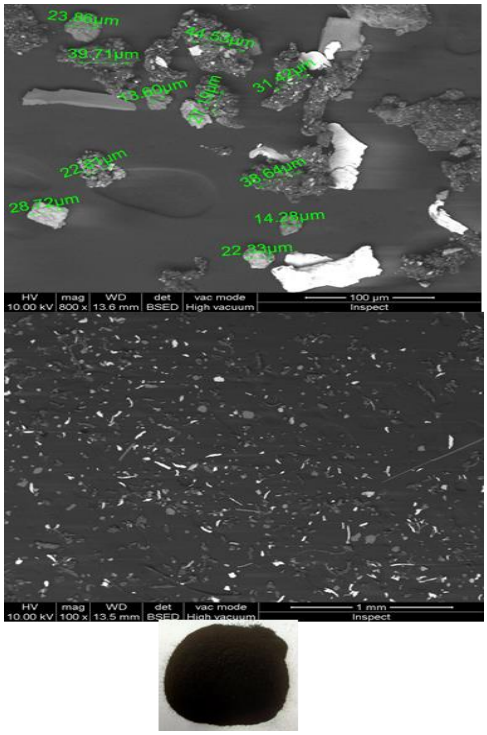

Fig. 4 Microstructures of micro rubber ash

Fig. 5 Dry mix for natural sand, LWFA, MRA and cement.

and MRA were investigated. Ten mixtures of lightweight rubberized mortar (LWRM) were prepared as follows: traditional cement mortar (control mixture), three mixes with different percentages of LWFA (25%, 50% or 75%),

Table 7 Mix proportions of lightweight rubberized mortar

Mix ID	LWFA %	MRA %	Cement (kg)	Natural sand (kg)	LWFA (kg)	MRA (kg)	w/c (kg)	SP (kg)
Control	----	----	1.0	3.0	---	---	0.40	0.03
M25%LWFA	25	----	1.0	2.25	0.255	---	0.42	0.03
M50%LWFA	50	----	1.0	1.5	0.509	---	0.44	0.03
M75%LWFA	75	----	1.0	0.75	0.764	---	0.45	0.03
M2.5%MRA	----	2.5	1.0	2.925	----	0.027	0.41	0.03
M5.0%-MRA	----	5.0	1.0	2.85	----	0.055	0.42	0.03
M7.5%-MRA	----	7.5	1.0	2.775	----	0.082	0.43	0.03
M25%LWFA+5%MRA	25	5	1.0	2.10	0.255	0.055	0.44	0.03
M50%LWFA+5%MRA	50	5	1.0	1.35	0.509	0.055	0.45	0.03
M75%LWFA+5%MRA	75	5	1.0	0.60	0.764	0.055	0.47	0.03

Fig. 6 Hydraulic testing machine 1500 KN capacity

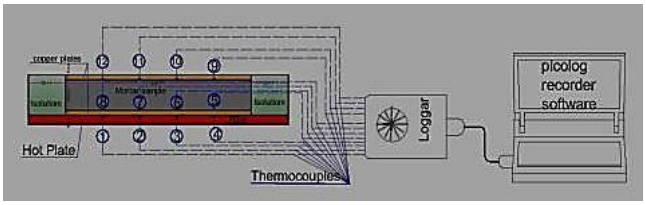

Fig. 7 Diagram of the thermal conductivity apparatus

three mixes with different percentages of MRA (2.5%, 5% or 7.5%) by volume (Trilok *et al.* 2014, Turatsinze and Garros 2008, İlker and Abdullah 2007), and three mixes consisting both types in determined ratios (25% LWFA+ 5% MRA, 50% LWFA+5% MRA and 75% LWFA+5% MRA). A high water-reducing addition was used (superplasticiser) by a percentage of 3% of cement content by weight, as presented in Table 7. The mixing steps were as follows: natural sand, LWFA, MRA and cement were mixed for 2 min (see Fig. 5); all dry mixtures were mixed using a superplasticiser and 60% of water for 4 min; and the mixtures were mixed for 5 min using residual water.

2.3 Testing procedure

2.3.1 Workability tests

Flow table test was carried out on fresh mortar mixes before they were cast. This step ensured the comparable flow ability for all mixes. The moulds used complied with EC 203-2016.

2.3.2 Unit weight

Unit weight measurements were carried out on the hardened samples of mortar on 70 mm × 70 mm × 70 mm cubes before the 28 day compressive strength tests with a sensitive balance. Unit weight was determined according to EC 203-2016.

2.3.3 Compressive and indirect tensile strength test

Compressive strength tests were performed for 7 and 28 days on 70 mm×70 mm×70 mm cubes according to EC 203-2016. The samples were cured in water for 28 days. All the specimens were tested in a hydraulic testing machine (MATEST) with a capacity of 1500 KN (see Fig. 6). Indirect tensile tests were performed for 28 days on 10 mm×20 mm cylinder according to EC 203-2016 (see Fig. 6). The samples were cured in water for 28 days. The ratio of compression strength to tensile strength LWRM with different replacement proportions of LWFA and MRA was obtained according to the experimental program.

2.3.4 Thermal conductivity (K-value)

Stable-case heat transfer test (see Fig. 7) clarified the test procedures and showed its dependency on the un-guarded copper hot plate technique, to calculate the K-value of the LWRM specimens. The well-mixed LWRM were placed in 25 mm×200 mm×400 mm slab-shaped test moulds. For the collection of data from the thermocouple, the type K thermocouple used was calibrated according to ASTM C 177.

The test setup was coordinated in a perpendicular path with a block of 5 mm-thick copper sheet, and four thermocouples were joined to the bottom and top surfaces by placing the test sample between an upper hot copper sheet and lower copper sheet (two sets of thermocouples were connected to the bottom surface). The four thermocouples attached beneath the bottom copper sheet recorded heat in the hot copper sheet. The four thermocouples attached on the upper surface of the bottom copper sheet recorded the heat at the surface connecting the upper surface of the bottom copper sheet and the bottom surface of the LWRM sample surface. The bottom copper sheet recorded heat at the surface connection between the copper sheet upper surface and the LWRM sample bottom surface. The four thermocouples attached on the lower surface of the top copper sheet recorded heat (temperatures) at the interface between the bottom surface of the upper copper sheet and the upper surface of the LWRM sample. Average temperatures were determined by the four thermocouples at four positions. The twelve thermocouples were linked to software (Picolog Recorder), which in turn was linked to a computer laptop for the recording of

Table 8 Results of phisical and hardened properties of lightweight rubberized mortar

Mix ID:	Flowability cm	Unit weight 28 days (Kg/m^3)	Compressive strength (MPa)				Tensile strength (MPa)			Thermal conductivity (k) (W/mK)
			7 days	28 days	Standard deviation at 28 days	coefficients of variation (%) at 28 days	28 days	Standard deviation at 28 days	coefficients of variation (%) at 28 days	
Control	20.2	2209.1	21.9	32.5	8.58	2.6	2.1	0.65	3.04	0.842
M25%LWFA	20.4	1822.3	14.1	21.2	10.21	4.8	1.4	0.64	4.55	0.611
M50%LWFA	20.7	1480.6	11.9	16.6	6.95	4.1	1.2	0.41	3.4	0.509
M75%LWFA	21.0	1115.1	7.3	11.4	4.89	4.2	0.9	0.4	4.53	0.412
M2.5%MRA	21.2	2170.4	21.4	28.2	9.39	3.3	2.1	0.8	3.88	0.712
M5.0%-MRA	21.6	2133.5	20.0	25.5	7.76	3.1	1.9	0.82	4.29	0.651
M7.5%-MRA	21.8	2100.2	16.4	22.8	6.13	2.6	1.7	0.77	4.64	0.582
M25%LWFA+5%MRA	21.8	1770.8	16.0	22.1	8.58	3.8	1.7	0.64	3.83	0.483
M50%LWFA+5%MRA	21.4	1407.5	14.2	19.9	8.16	4.1	1.7	0.28	1.68	0.402
M75%LWFA+5%MRA	21.7	1041.3	7.1	10.2	4.89	4.8	0.9	0.41	4.53	0.316

Fig. 8 Dry shrinking test device

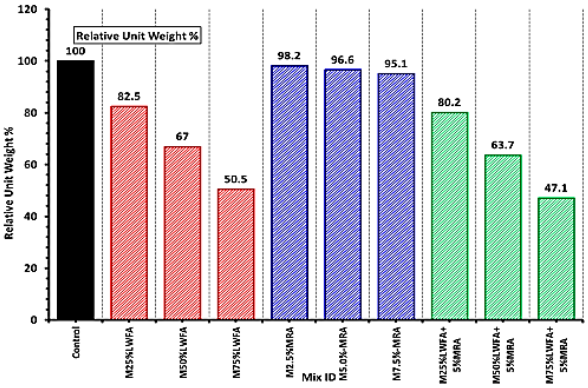

Fig. 9 Relative unit weight of LWRM compared to the control mix

temperatures at twelve points, as presented in Fig. 7. The samples were tested for approximately 5 h or 1 h when temperature was lower than a 0.2°C. The copper sheet K-value was used in performing heat transfer computation, as well as the K-value of an LWRM sample, (Q) as Eq. (1)

$$Q = (kc).(Ac).\frac{\Delta Tc}{\Delta Xc} \qquad for\ copper \qquad (1)$$

where Ac=area (m^2) for the copper sheet; ΔX_c=thickness (m) for the copper sheet; Q=heat transfer (W) through the copper sheet; ΔT_c=temperature difference (°C) for copper sheet; and kc=thermal conductivity (K-value; W/mK) of the copper sheet. According to the recorded average temperatures within steady-state conditions for the upper and lower sides of the LWRM sample, thermal conductivity (K-value) in the LWRM samples can be calculated using Eq. (2)

$$\text{km} = \frac{Qc\ .\Delta Xm}{Am\ .\Delta Tm} \qquad (2)$$

where Am=the area (m^2) for LWRM; ΔX_m=the thickness (m) for LWRM; Q_c=heat transfer (W; through the copper sheet and through the LWRM sample), as shown in Eq. (1); ΔT_m=temperature difference (°C) across the LWRM; and km = thermal conductivity (K-value; W/mK) of LWRM.

2.3.5 Dry shrinking test

The well-mixed LWRM were placed in 20 mm×20 mm×270 mm prism-shaped test moulds. The shrinkage heads, made of copper nails, were fixed in the surfaces of the two-end holes of the test samples and protruded by 8±1 mm from the ends of the test moulds. The moulds were removed after being cured in water for 7 days at 20±2°C. The initial lengths of the samples were measured along the determined direction after the calibration process for the apparatus, as shown in Fig. 8. The LWRM samples were left to stand at room temperature (20±2°C) and relative humidity (60%±5), then increase in the length of each sample was measured every 7 days for 91 days.

3. Discussions

3.1 Workability

The flow ability of mortars was kept constant at 22±2 cm in the LWRM samples containing LWFA and MRA. The results are displayed in Table 8. The data showed little fluctuations, depending on the LWFA dosages used and MRA and on the water quantity used in the mixing. Thus, at a low LWFA dose, the resulting mortars had decreased air void content and required low amounts of water for them to exhibit workability.

3.2 Hardened properties of LWRM

The LWRM hardened properties results are studied. Table 8 presents the results obtained from laboratory tests, such as unit weight, compressive strength, tensile strength and thermal conductivity.

3.2.1 Unit weights

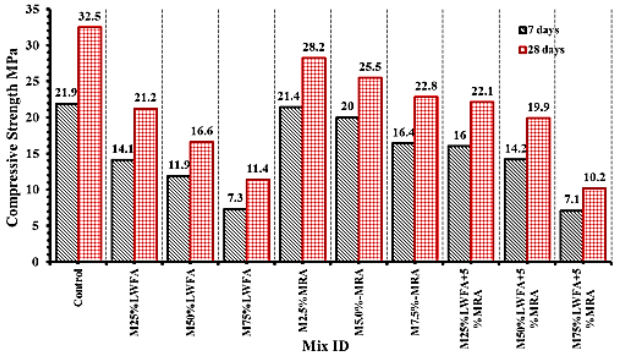

Fig. 10 Compressive strength of LWRM at 7 and 28 days

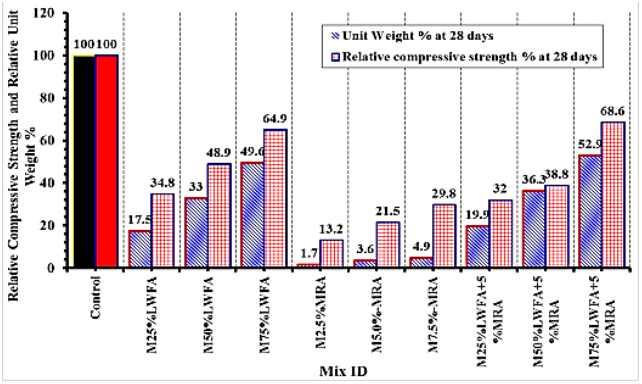

Fig. 11 Relationship between relative compressive strength % and relative unit weight % for LWRM compared to the control mix

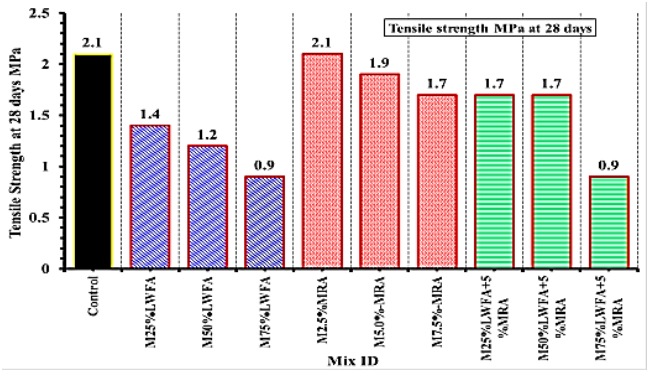

Fig. 12 Tensile strength of LWRM compared to the control mix

The unit weights of all the LWRM mixtures were measured. Fig. 9 presents the relative unit weight (%) the of hardened states. The unit weights of the mixes ranged from 2209 kg/m^3 to 1041 kg/m^3 at 28 days. The experimental results showed that the unit weights of the LWRM samples decreased when the percentage of LWFA increased. The unit weights of the mixes using LWFA at 25%, 50% or 75% in a hardened state result were lower than the unit weight of the control mix by approximately 17.5%, 33% or 49%, respectively. The decrease in the unit weight of mortar with LWFA can be related to the high decrease in specific gravity and increase in the amount of internal voids, as shown in the microstructure scans in Fig. 3, Fig. 18(b) and Figs. 19(a)-(b) compared with those in natural sand, as in shown in the SEM images in Fig. 18(a). Similarly, unit weight decreased when MRA was used as a replacement for natural sand, but the effect on weight loss was slightly less significant. The unit weights of the mixes using MRA at 2.5%, 5.0% or 7.5% in a hardened state slightly decreased compared with the unit weight of the control mix by approximately 2%-5%. Moreover, The unit weights of the mixes using LWFA and MRA at the following proportions: 25%LWFA+5%MRA, 50%LWFA+5%MRA and 75%LWFA+5%MRA decreased compared with the unit weight of the control mix by approximately 20%-53%. The major reason for the decrease in the unit weight of LWRM was the high air content due to the high porosity of the LWFA and MRA surfaces, which tend to keep air internal. Air content, which decreased in unit weight, increased with the quantities of LWFA and MRA,this result agreed with (Ayesha *et al.* 2019, Tayfun and Ilker 2010).

3.2.2 Compressive strength of LWRM

Fig. 10 shows the compressive strength of each LWRM mixture at 7 and 28 days. The use of LWFA and MRA as replacements for natural sand had an unfavourable effect on compressive strength, especially when the replacement ratios of LWFA or MRA were high. The experimental results showed that the compressive strength of the LWRM decreased when the percentage of LWFA increased. The compressive strength of mixes using LWFA at 25%, 50% and 75% were lower than that of the control mix by approximately 34.7%-64.9%, as shown in Fig. 10. Decrease in the compressive strength of mortar containing LWFA can be related to the high porosity and lowered specific gravity compared with those of natural sand. Similarly, compressive strength decreased when MRA was used, but the effect on compressive strength was lower than the effects of the LWFA mixtures. The compressive strength of the mixes using MRA at 2.5%, 5.0% and 7.5% decreased compared with that of the control mix by approximately 13.2%-29.8%, as shown in Fig. 10. Moreover, The compressive strengths of the mixes between LWFA and MRA with the following proportions: (25%LWFA+5%MRA), (50%LWFA+5%MRA) and (75%LWFA+5%MRA) decreased in the compressive strength compared with the control mix by approximately 32%-68.6%, as shown in Fig. 10. The major reason for the decrease in the compressive strength of LWRM was the high content of porosity and internal air, as shown in the SEM images. Air content increased with the quantities of LWFA and MRA and caused a decrease in compressive strength. By contrast, the LWFA or MRA or their mixtures at determined ratios (LWFA+MRA) exerted positive effects on reduced unit weight, K-value and dry shrinkage, as shown in the listed results and Fig. 11. Generally, the LWRM used in plasterwork or in the isolation of the last roofs of buildings cannot be considered a load-carrying element in buildings. Therefore, isolating roofs can be considered another major property of LWRM apart from unit weight, thermal K-value and dry shrinkage.

3.2.3 Tensile strength

Table 8 and Fig. 12 present the effects of LWFA and

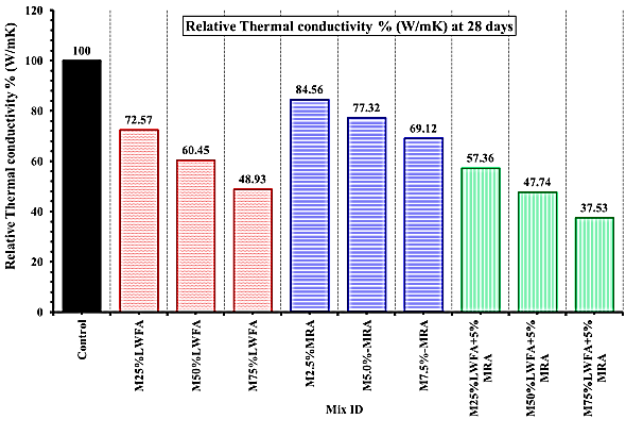

Fig. 13 Relative thermal conductivity (%) of LWRM compared to the control mix

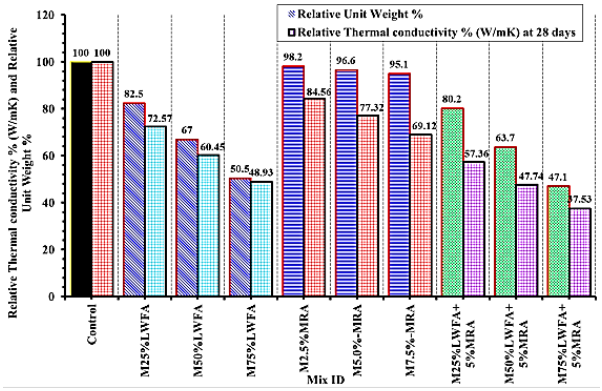

Fig. 14 Relationship between relative thermal conductivity % and relative unit weight % for LWRM compared to the control mix

MRA on tensile strength. Reduction in tensile strength was observed in all the samples. In the control mixture specimens, tensile strength decreased from 5.7% to 75.62% when replacement content (LWFA+MRA) increased from 25% to 100%. At 28 days, the tensile strength of the control mix was 2.1 MPa. Fig. 12 shows the effects of LWFA, MRA and LWFA+MRA mixtures on the 28 day tensile strength of LWRM. The tensile strength reduced gradually with the increase of LWFA or MRA or mixture between both contents. The replacement percentages (25%, 50% and 75%) of NA with LWFA decreased tensile strength from 33% to 57.1% at 28 days. The replacement percentages 2.5%, 5.0% and 7.5% of NA with MRA decreased tensile strength from 0% to 19% at 28 days. Moreover, The tensile strength of the mixes using LWFA and MRA at the following proportions: (25%LWFA+5%MRA), (50%LWFA+5%MRA) and (75%LWFA+5%MRA) decreased from 19% to 57.1% at 28 days. This result is compatible with the result in the literature (Yu and Zhu 2016).

3.2.4 Thermal conductivity (K-value) of LWRM

Fig. 13 and Table 8 present the K-values. The heat transfer rates in the LWRM specimens incorporating LWFA and MRA decreased compared with those of the control mixes (0.842 W/mK). This value was reduced to 0.316 W/mK when the mixture containing 75% LWFA and 5% MRA was used. The relative percentages of K-value in the samples with LWFA or MRA with different proportions or their mixtures compared with percentage of the control sample are presented in Fig. 13. The K-value of LWRM decreased in all the specimens compared with that of the control specimen. The results indicated that the samples without MRA containing 25%, 50% and 70% LWFA had relative K-values of 72.57%, 60.45% and 48.93%, respectively compared with the K-value of the control sample (100%). Relative K-values of 84.56%, 77.32% and 69.12% were considered 100%. Adding 5% MRA to the LWRM containing LWFA 25%, 50% and 75% resulted in relative K-values of 57.36%, 47.74% and 37.53% compared with the control sample considered 100%. Thus, the K-value of LWRM decreased when the amount of LWFA or MRA increased. Moreover, the K-value of LWRM

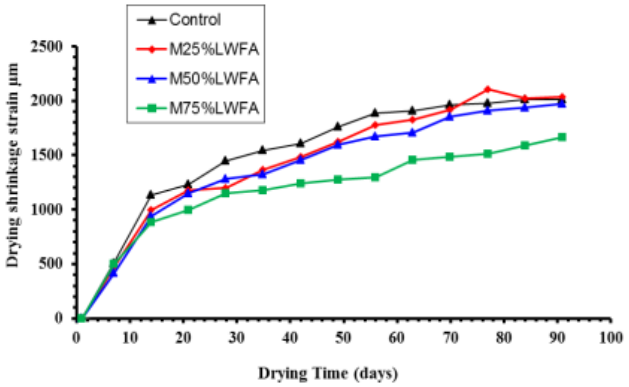

Fig. 15 Drying shrinkage of LWRM at 25%, 50% and 75% LWFA

decreased with unit weight (see Fig. 14). The major reason beyond the decrease in the K-value of LWRM was due to the high porosity and amount of internal air, as shown in the microstructure scans in Fig. 18(b) and Figs. 19(a)-(b). Air content increased with the quantities of LWFA and MRA and caused a decrease in compressive strength, as indicated by the microstructure images of LWFA and MRA (see Figs. 3-4, respectively). This result is compatible with the result in the literature (Pania *et al.* 2012, Widodo *et al.* 2017).

3.2.5 Drying shrinkage of LWRM

The drying shrinkage of the LWRM decreased when the percentage of LWFA increased. The lowest drying shrinkage values were obtained when the mixes using LWFA at 25%, 50% and 75% were used, as shown in Fig. 15. The rate of shrinkage decreased with decreasing aggregate density and increasing aggregate porosity (Min-Hong *et al.* 2005). Fig. 16 presents the deformation of drying shrinkage of the LWRM mixed with different percentages of MRA particles. A slight change in the drying shrinkage of LWRM was observed when MRA particles were mixed with the mortar. The drying shrinkage of LWRM slightly decreased significantly with increasing amount of MRA in the mixes (Tayfun and Ilker 2010, Canova *et al.* 2012) reported that the drying shrinkage of self-consolidating mortars with 10%, 20% and 30% scrap rubber content is lower than that of control self-

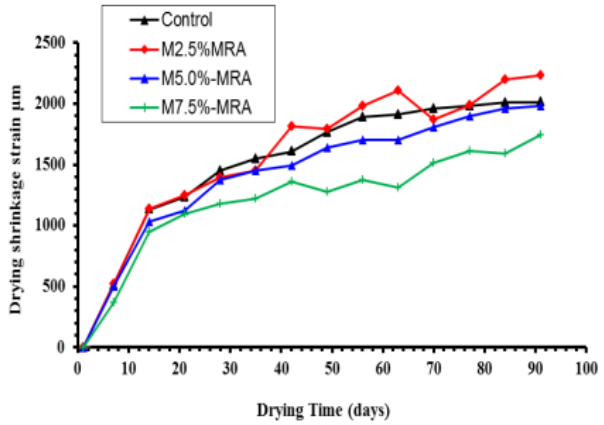

Fig. 16 Drying shrinkage of LWRM at 2.5%, 5% and 7.5% MRA

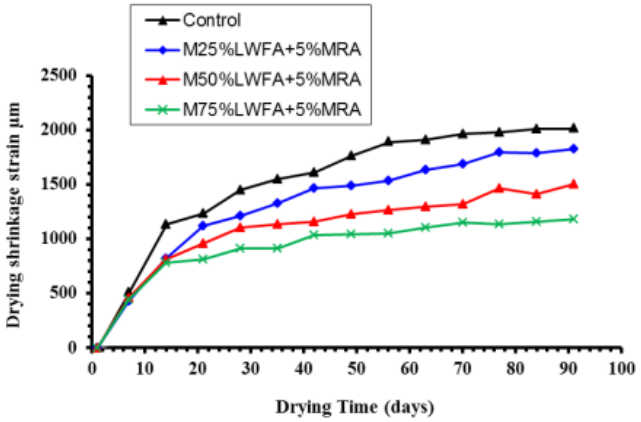

Fig. 17 Drying shrinkage of LWRM at (25%+5%), (50%+5%) and (75%+5%) (LWFA+MRA)

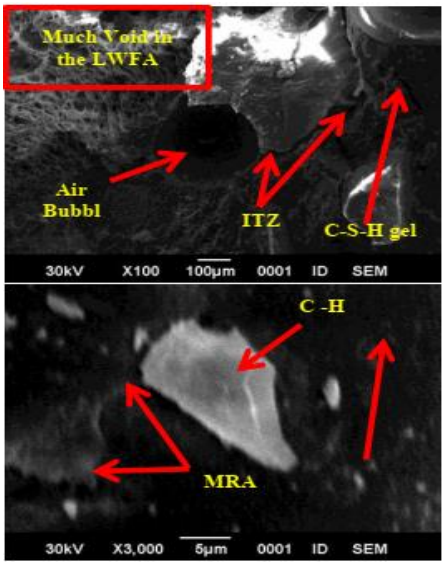

(a) control mix

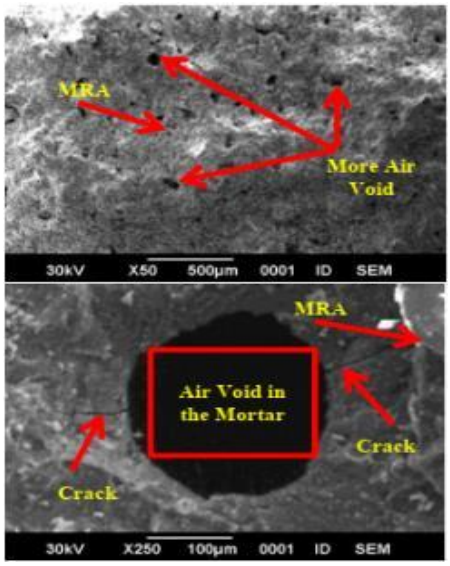

(b) 50% LWFA replacement from natural sand

Fig. 18 Scanning electron microscopy for LWRM

consolidating mortars. The LWFA and MRA particles retained water between their layers and surfaces in the cement mortar, thereby reducing the dry shrinkage of LWRM. Moreover, the drying shrinkage values of the mixes using LWFA and MRA at different proportions (25%LWFA+5%MRA, 50%LWFA+5%MRA and 75%LWFA+5%MRA) decreased compared with the drying shrinkage of the control mix, as shown in Fig. 17. The major reason for the decrease in the drying shrinkage of LWRM was the high porosity and internal air in the lightweight fine aggregate, as may be observed from the microstructure images of LWFA (see Fig. 3). Moreover, owing to the high porosity of LWFA and a little content of MRA particles, the dry shrinkage for LWRM was reduced**.**

3.2.6 Scanning electron microscopy images

Fig. 18(a) shows the SEM images of the control mix (cement mortar specimen). As shown in Fig. 18(a), the cement mortar specimen (control mix) was denser than the mixtures containing LWFA or MRA. Fig. 18(b) displays an SEM image for a lightweight mortar specimen. As shown in Fig. 18(b), lightweight mortar contained many voids and showed a good bond between LWFA and cement paste. Fig. 19(a) displays the SEM image of a rubberized mortar specimen. The MRA is the tight and short lines distributed in the entire mixture. The rubber particles poorly bonded with the surrounding paste of cement and this characteristic was the main reason for the poor strength performance of the mix containing MRA. The black point in the center of the image was an MRA particle, and a weak bond with the surrounding paste of cement was observed. The SEM images displayed a good bond between MRA particles and cement paste. A micro-crack in the ITZ microstructure of LWRM in the mix containing MRA is shown in Fig. 19(a). The amount of MRA may be responsible for this result. This characteristic is the main reason for the poor strength performance of the mix containing MRA. In the SEM images of the LWRM mixtures, the effects of the 25%, 50% and 75% LWFA replacement percentages on the microstructures were more obvious compared with the effect of the control mix. The SEM images of the LWRM specimens containing 50%LWFA+5%MRA replacement

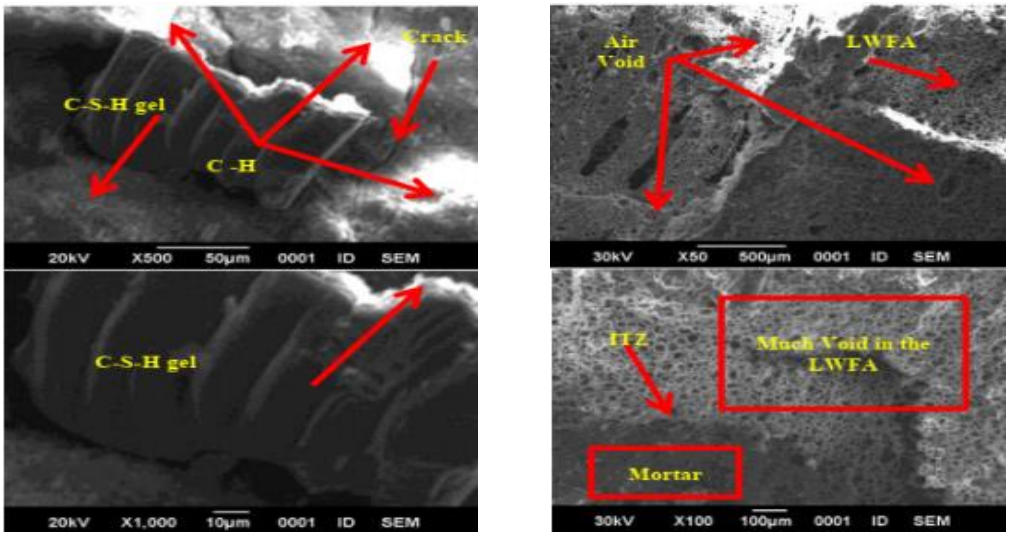

(a) 5% MRA replacement from natural sand (b) 50%LWFA+5%MRA replacement from natural sand

Fig. 19 Scanning electron microscopy for LWRM

(see Fig. 19(b)) contained more porous structures than the image of the control mix, and the percentages of the voids increased with the replacement level for natural sand to up to 75%, as displayed in Fig. 18(b) and Fig. 19(b). Basing on the microstructure, we can conclude that a large amount of voids in the samples containing MRA or LWFA or their mixtures may be the reason for the decrease in heat transfer in the plaster mortar samples. This result is compatible with the results in the literature (Pania *et al.* 2012).

4. Conclusions

This study studies the effect of MRA on the K-value of cement mortar. The following conclusions were obtained:

- Flow ability test data showed small fluctuations, which depended on LWFA dosage, and the flow ability of mortars was approximately 22±2 cm.
- Experimental results showed that unit weight of the LWRM decreased when the percentages of LWFA and MRA increased.
- The compressive strength decreased by approximately 64% and 29% when 75% LWFA and 5% MRA were used, respectively, compared with that of the control specimens.
- The tensile strength decreased by approximately 57% and 19% when 75% LWFA and 5% MRA were used, respectively, compared with that of the control specimens.
- The K-value of LWRM decreases with decreasing in the unit weight of mortar.
- The K-value of LWRM ranged from 0.316 W/mK to 0.712 W/mK compared with that of traditional mortar (0.842 W/mK). When LWFA content increased in the mixtures, the K-values decreased. The enhancement in the thermal insulation of LWRM showed that this type of mortar is a potential exterior plaster material for isolating the last roofs of buildings and enveloping systems of buildings.
- The drying shrinkage test results showed that drying shrinkage for LWRM slightly decreased at mix up between LWFA and MRA content (75% LWFA+5% MRA).
- The SEM analysis results showed the good distribution of LWFA, MRA and air voids in the LWRM mixes. This distribution led to decreases in the unit weight, thermal conductivity and drying shrinkage of the mortar mix compared with those of the control mix.
- LWRM used in the plaster work or isolation cannot be considered a load-carrying element in buildings. Therefore, physical and thermal properties, such as unit weight, drying shrinkage and K-value, can be considered the major advantages of LWRM. The LWRM containing LWFA and MRA can be used as engineering surface plaster and may be useful in solving cracking issues in the conventional surface of mortar plaster and enhancing external heat isolation.

Recommendations for future studies

- Study the effect of water and humidity on the durability of rubberized mortar.
- Study the effect of water absorption, permeability on the durability properties of rubberized mortar.

Acknowledgements

I sincerely thank the laboratory of Civil Constructions Dep., Faculty of Technology and Education, Suez University, Egypt for funding support. The assistance of Ph.D. students, Mostafa Helmy Gresh and Nour Bassem Farhat, in carrying out some of the experimental work is also acknowledged. Also, I sincerely thank the MARSO Rubber Company, 10th of Ramadan City, Egypt.

References

Alaloul, W.S., Musarat, M.A., Tayeh, B.A., Sivalingam, S., Rosli, M.F.B., Haruna, S. and Khan, M.I. (2020), "Mechanical and deformation properties of rubberized engineered cementitious composite (ECC)", *Case Stud. Constr. Mater.*, **13**, 1-13. https://doi.org/10.1016/j.csc m.2020.e00385.

Albano, C., Camacho, N., Reyes, J., Feliu, J.L. and Herna, N.M. (2005), "Influence of scrap rubber addition to Portland I concrete composites: destructive and non-destructive testing", *Compos. Struct.*, **71**, 439-446. https://doi.org/10.1016/j.compstr u c t.2005.09.037.

Ali, A., Aliabdo, A.M. and Abd-Elmoaty, H.H.H. (2013), "Utilization of crushed clay brick in cellular concrete production", *Alex. Eng. J.*, **53**, 119-130. http://dx.doi.org/10.1016/j.aej.2013.11.005.

ASTM (2009), C150. Standard Specification for Portland Cement.

ASTM (2017), C494/C494M-17, Standard Specification for Chemical Admixtures for Concrete.

ASTM (2020), C897-15, Standard Specification for Aggregate for Job-Mixed Portland Cement-Based Plasters.

ASTM C177-19, Standard Test Method for Steady-State Heat Flux Measurements and Thermal Transmission Properties by Means of the Guarded-Hot-Plate Apparatus, ASTM International, West Conshohocken, PA.

Ayesha, S., Abdullah, Md., Rayed, A., Mugahed, A.Y.H. and Farhad, A.H.A. (2019), "Properties and utilizations of waste tire rubber in concrete: A review", *Constr. Build. Mater.*, **224**, 711-731. https://doi.org/10.1016/j.conbuil dm at.2019.07.108.

Canova, J.A., Bergamasco, R., Angelis Neto, G.D. and Gleize, P.J.P. (2012), "Comparative analysis of the properties of composite mortar with addition of rubber powder from worn tires", *Ambiente Construído*, **12**(1), 257-267. https://doi.org/10.1590/S1678-86212012000100017.

ECP 203-2016 (2016), Egyptian Code, Housing and Building Research Center, Cairo, Egypt.

Egyptian Standard Specification ESS (2009), No. 4756.

Fadiel, A., Al Rifaie, F., Abu-Lebdeh, T. and Fini, E. (2014), "Use of crumb rubber to improve thermal efficiency of cement-based materials", *Am. J. Eng. Appl. Sci.*, **7**, 1-11. https://doi.org/10.3844/ajeassp.2014.1.11.

Hunag, L., Wang, H. and Wang, S. (2015), "A study of the durability of recycled green building materials in lightweight aggregate concrete", *Constr. Build. Mater.*, **96**, 353-359. https://doi.org/10.1016/j.conbuildmat.2015.08.018.

İlker, B.T. and Abdullah, D. (2007), "Durability of rubberized mortar and concrete", *J. Mater. Civil Eng.*, **19**, 173-178. https://doi.org/10.1061/ASCE0899-1561200719:2173.

Jie, Y., Jun, W., Feng, X., Hao, L. and Yunzhang, L. (2019), "Assessment of building external wall thermal performance based on temperature deviation impact factor under discontinuous radiant heating", *J. Therm. Sci.*, **28**, 1129-1140. https://doi.org/10.1007/s11630-019-1173-x

Khaloo, A.R., Dehestani, M. and Rahmatabadi, P. (2008), "Mechanical properties of concrete containing a high volume of tire-rubber particles", *Waste Manage.*, **28**, 2472-2482. https://doi.org/10.1016/j.wasman. 2008.01.015.

Li, Z. and Li, X. (2007), "Development of thermal insulation materials with granular phase change composite. In: Advances in construction materials", *Berlin Heidelberg*, 741-748. https://doi.org/10.1007/978-3-540-72448-3_75.

Min-Hong, Z., Lian, L. and Paramasivam, P. (2005), "Shrinkage of high-strength lightweight aggregate concrete exposed to dry environment", *ACI Mater. J.*, **102**(2), 86-92.

Mohamadien, H.A., Hassan, H.M., Ibrahim, O.M.O. and Assi, L.N. (2019), "Effect of micro rubber ash on the properties of self-compacting concrete", *Int. J. Eng. Sci. Res. Technol.*, **8**, 209-225. https://doi.org/10.5281/zenodo.3540376.

Najim, K.B. and Hall, M.R. (2012), "Mechanical and dynamic properties of self-compacting crumb rubber modified concrete", *Constr. Build. Mater.*, **27**, 521-530. https://doi.org/10.1016/j.conbuildmat.2011.07.013.

Official Website of MREPCS, Malaysian Rubber Cxport Promotion Council.

Pania, M., Xi, Y. and Li, Y. (2012), "Utilization of phase change materials and rubber particles to improve thermal and mechanical properties of mortar", *Constr. Build. Mater.*, **28**, 713-721. https://doi.org/10.1016/j.conbuildmat .2011.10.039.

Richardson, A., Heniegal, A. and Tindall, J. (2017), "Optimal performance characteristics of mortar incorporating phase change materials and silica fume", *J. Green Build.*, **12**, 59-79. https://doi.org/10.3992/1943-4618.12.2.59.

Saber, H. (2012), "Investigation of thermal performance of reflective insulations for different applications", *Build. Environ.*, **52**, 32-44. https://doi.org/10.1016/j.builden v.2011.12.010.

Sharkawi, A.E. (2015), "Performance of lightweight mortar made of locally available sustainable aggregate", *15th International Conference on Advances in Structural and Geotechnical Engineering, ICASGE*, Hurghada, Egypt, 1-14.

Sofi, A. (2018), "Effect of waste tyre rubber on mechanical and durability properties of concrete-A review", *Ain Shams Eng. J.*, **9**, 2691-2700. https://doi.org/10.1016/j. a sej.2017.08.007.

Tarabieh, K. and Aboulmagd, A. (2019), "Thermal performance evaluation of common exterior residential wall types in Egypt", *Build.*, **9**, 1-15. https://doi.org/10.3390/buildings9040095.

Tayfun, U. and Ilker, B.T. (2010), "The role of scrap rubber particles on the drying shrinkage and mechanical properties of self-consolidating mortars", *Constr. Build. Mater.*, **24**, 1141-1150. https://doi.org/10.1016/j.conbuildmat.2009.1 2.027.

Topçu, I. (1995), "The properties of rubberized concretes", *Cement Concrete Res.*, **25**(2), 304-310. https://doi.org/10.1016/0008-8846(95)00014-3.

Trilok, G., Sandeep, C. and Ravi, K.S. (2014), "Assessment of mechanical and durability properties of concrete containing waste rubber tire as fine aggregate", *Constr. Build. Mater.*, **73**, 562-574. http://dx.doi.org/10.1016/j.conbuild mat .2014.09.102.

Turatsinze, A. and Garros, M. (2008), "On the modulus of elasticity and strain capacity of Self-Compacting Concrete incorporating rubber aggregates", *Resour. Conserv. Recyc.*, **52**, 1209-1215. https://doi.org/10.1016/j.resconrec.2008.06.0 12.

Widodo, S., Maarif, F. and Gan, B.S. (2017), "Thermal conductivity and compressive strength of lightweight mortar utilizing pumice breccia as fine aggregate", *Procedia Eng.*, **171**, 768-773. https://doi.org/10.1016/j.proeng.2 017.01.446.

Yu, Y. and Zhu, H. (2016) "Influence of rubber size on properties of crumb rubber mortars", *Mater.*, **9**, 1-12. https://doi.org/10.3390/ma9070527.

Yu, Y. and Zhu, H. (2019), "Effects of rubber size on the cracking resistance of rubberized mortars", *Mater.*, **12**, 1-12. https://doi.org/10.3390/ma12193132.

CC